This article has been accepted for publication in a future issue of this journal, but has not been fully edited. Content may change prior to final publication. Citation information: DOI 10.1109/TMC.2018.2822279, IEEE Transactions on Mobile Computing

Traffic-Aware Efficient Mapping of Wireless Body Area Networks to Health Cloud Service Providers in Critical Emergency Situations

Sudip Misra, *Senior Member, IEEE,* and Amit Samanta, *Student Member, IEEE*

Abstract—In a post-disaster situation, increased concentration of patients in an area increases the traffic load of the network significantly, which degrades its performance with respect to mapping cost and network throughput. Therefore, to manage the increased traffic load and to provide ubiquitous medical services, we propose a disease-centric health-care management system using wireless body area networks (WBAN) in the presence of multiple health-cloud service providers (H-CSP). The theory of Social Network Analysis (SNA) is adopted to optimize the computational complexity and the traffic load of the network in an area, considering different disease types and the criticality indices of the WBANs. In such a scenario, Disease-centric Patient Group (DPG) formation among coexisting WBANs ensures optimized traffic load and reduced computational complexity. However, the formation of DPG alone is not sufficient to provide Quality-of-Service (QoS) to each WBAN. Therefore, to address these issues, we formulate a pricing model for the efficient mapping of critical WBANs from a DPG to a H-CSP to optimize the expected packet delivery delay and the network throughput. Consequently, to identify the critical WBANs from a DPG, we design a decision parameter based on an assortment of selection parameters. The performance of the Efficient Healthcare Management (HCM) scheme is analyzed based on distinct measures such as cost effectiveness, service delay, and throughput. Simulation results exhibit significant improvement in the network performance over the existing schemes.

Index Terms—Wireless Body Area Networks, Cloud Computing, Disease-centric Patient Grouping, Heterogeneous Health Cloud Service Provider, Quality of Service, Energy Efficient, Traffic Aware, Efficient Mapping

1 Introduction

In a post-disaster situation, monitoring of affected patients in an area and providing them with reliable and ubiquitous electronic healthcare services, is a major challenge [1]. Therefore, to manage such situations, a cloud-assisted WBAN architecture provides cost-effective and real-time services to the affected victims. Cloud-assisted WBAN is an infrastructural and systematic integration of traditional WBAN with cloud [2]. In a conventional WBAN architecture [3]–[5], the body sensors located in the vicinity of human tissue sense the physiological signals of the patients, process them, and then send the sensed information to the Local Processing Unit (LPU). The LPU sends the medical data to the servers through the local APs for analysis by the medical experts. In case of cloud-assisted WBANs, the local APs send the medical data directly to the *health cloud service provider* (H-CSP). Therefore, WBAN equipped patients can get cost-effective and ubiquitous electronic healthcare services in a critical emergency situation. Further, a cloud-assisted WBAN provides adequate services for wide ambulatory and sports applications [6], [7].

Motivation: Increased number of WBANs in a specific area degrades the performance of each WBAN in terms of end-to-end packet delivery delay and network throughput. Therefore, the management of increased traffic load of WBANs is a major challenge, as each WBAN carries sensitive medical data. In a conventional WBAN architecture, medical data specific to a particular disease is dedicatedly stored in a particular server to manage the data efficiently. Therefore, when specific disease-affected patients are not present in that area, then these servers become unutilized and the network management cost increases. In this context, the integration of cloud services to a WBAN platform provides cost effective, elastic and real-time healthcare services [8]. Due to the use of cloud services, if the WBANs specific to particular diseases are not present in that area, cloud services can be utilized by giving the same to other WBANs. In normal situations, resource demand from each WBAN may differ, which may even increase during emergencies. Due to the fact that different disease-specific WBANs demand different kinds of services, each such WBAN needs to choose an optimal H-CSP among heterogeneous cloud service providers.

Contribution: Our work attempts to identify the problem of traffic load minimization and selection of an optimal H-CSP pricing policy for heterogeneous WBANs in a cloud-enabled platform. A cloud infrastructure provides resources on requirement to a WBAN in an ubiquitous manner. Each WBAN can store medical data, depending upon the patients' medical situations, without being deeply concerned about the infrastructure of the cloud [9]. This means that a WBAN attempting access to resources may not deploy its own resource infrastructure and even may not be aware of the physical presence of the deployed infrastructure. The cloud users only pay for the amount of resources used by them for a specified time period. Thus, it leads to an overall resource optimization due to sharing of resources and reduction in the overall cost of usage. The major *contributions* of this manuscript are discussed as follows :

i) Disease-centric patient grouping is considered, depending on the syndrome associated with these diseases such as epidemic cholera, glandular fever, and epidemic parotitis, to minimize the computational complexity and traffic load for epidemic emergency situation in a hospital environment.
ii) The work focuses on the optimal mapping of critical

S. Misra, and A. Samanta are with the Department of Computer Science and Engineering, Indian Institute of Technology, Kharagpur, 721302, India, Email: {smisra, amitsamanta}@sit.iitkgp.ernet.in

This article has been accepted for publication in a future issue of this journal, but has not been fully edited. Content may change prior to final publication. Citation information: DOI 10.1109/TMC.2018.2822279, IEEE Transactions on Mobile Computing

WBANs to a particular H-CSP among several heterogeneous H-CSPs, based on the capacity, robustness, and capacity in terms of available resources, service delay and pricing policy of the H-CSPs.

iii) The proposed solution also maintains the energy efficiency of each WBAN belonging to a particular DPG in the presence of heterogeneous H-CSP.

The manuscript is organized as follows. In Section 2, we crisply discuss the existing works on cloud-assisted WBANs. Section 3 describes the system and mathematical model of the proposed scheme. In Section 5, we propose an optimization problem for energy-efficient social relation grouping to optimize the traffic load of WBANs. Section 6 presents the optimal pricing policy in the presence of heterogeneous H-CSPs. Section 8 presents the simulation results and Section 9 discuss the future works.

2 Related Work

WBANs are used to monitor physiological parameters of a community of people. They produces huge volumes of medical data packets [10]. To store, analyze, and process such data, cloud computing provides adjustable storage and processing infrastructure to analyze the data streams generated in WBANs for both online and offline algorithms.

In this domain, Giancarlo *et al.* proposed a SaaS-based approach for building a community of WBANs to support cloud-assisted WBAN applications, named BodyCloud [11]. BodyCloud is an application-level infrastructure to integrate cloud and medical resources having multi-tier. Similarly, Fortino *et al.* [2] deployed cloud-assisted WBANs and identified the important issues, which are required to be solved for advancement and execution in advanced healthcare. This present system is overviewed and wrapped based on the necessities of creating efficient cloud-assisted WBAN architecture. Consequently, Quwaider *et al.* [12] proposed a novel cloudlet-based for productive data aggregation in WBANs. In this work, the authors focused on a large-scale data-generating WBANs to be available to the end-user or to the service provider in a reliable manner. Additionally, Zhang *et al.* proposed adaptive map-reduced framework to scale the capability of cloud resources for real-time applications [13]. In order to address these challenges, Chen *at al.* proposed the integration of WBANs with Long Term Evolution (LTE) infrastructure, to support high user mobility [14]. They also proposed an efficient scheme, termed as *named data networking* (*NDN*) to support rich and adaptive media streaming for healthcare content size suitability with low-cost and bandwidth saving. Due to the energy constrained nature of the body sensors, the huge amounts of packets aggregated by the WBANs necessitates powerful and secure storage, and an efficient query processing mechanism, while considering both real-time and energy constraints of WBANs. Diallo *et al.* [15] proposed a new architecture that integrates statistical modeling technologies into cloud-based WBANs, to maintain privacy for storage infrastructure and to minimize the overhead of real-time user query processing. Due to the huge volume of generated data and their long-term processing, the computational power and energy consumption of the data centers increases tremendously. Rachkidi *et al.* proposed a cooperative approach between WBANs and H-CSPs for efficient provisioning of health services in health-cloud to minimize service latency [16].

In a post-disaster scenario, it is important to aggregate physiological sensor data in an efficient manner, and channelized them to the cloud platform with minimum delay. Abbas *et al.* proposed personalized healthcare services for disease risk management using cloud services [17]. Additionally, Prasad *et al.* [18] proposed an optimal resource management scheme in cloud infrastructure using Auction mechanism. Zhou *et al.* proposed a blind online scheduling approach for mobile cloud environments to assign available severs based on the users request [19]. Samanta *et al.* [20] proposed an efficient architecture with varying traffic in an epidemic medical emergency situation. In this work, they proposed to form Relational Patient Group (RPG), depending on different disease types and syndromes. Similarly, Samanta *et al.* proposed a joint dynamic resource allocation and load balancing scheme for WBANs in the presence of poor link-quality [21]–[23]. Additionally, Ibarra *et al.* proposed a joint power and QoS control for energy-harvesting in WBANs [24]. Chen *et al.* proposed a novel robotics and cloud-assisted healthcare system to provide pervasive healthcare services, especially for mental diseases [25]. Kulkarn *et al.* also proposed optimized mobile cloud service architecture for real-time healthcare services [26].

Synthesis: Based on the review of existing literature, we infer that the existing works did not consider the problem of disease-centric electronic healthcare services to WBANs in multiple H-CSP environments, while the utility of each WBAN is optimal and the computational complexity decreases. We propose an architecture for offering disease-centric helathcare services using SNA [27] in a cloud-assisted WBAN architecture. Additionally, we consider the criticality index of WBANs to provide reliable and efficient medical services to medically emergent patients in real-time.

3 System Model

In a cloud-assisted WBAN architecture, $N = \{1, 2, \cdots, n\}$ a set of WBANs, $\mathcal{B} = \{B_1, B_2, \cdots, B_n\}$, are present in an area, to monitor the physiological condition of the patients, where each WBAN is composed of a set $M = \{1, 2, \cdots, M\}$ of heterogeneous body sensors, $B = \{b_1, b_2, \cdots, b_m\}$, which are connected to an LPU to aggregate the heterogeneous medical data from each body sensor [28], [29]. Due to the heterogeneity of the body sensors, each such sensor has different bandwidth requirement, $\mathcal{B} = \{\mathcal{B}_1, \mathcal{B}_2, \cdots, \mathcal{B}_m\}$, to transmit its data effectively. As each body sensor requires different bandwidth, each WBAN demands different aggregated bandwidths, $BW \in \{BW_1, BW_2, \cdots, BW_n\}$, to transmit its data from a specific H-CSP. Therefore, to fulfill individual requirements, each WBAN B_i connects to K number of heterogeneous H-CSPs, $\mathcal{C} = \{C_1, C_2, \cdots, C_k\}$, to achieve ubiquitous health services. The communication between sensor nodes to LPUs and LPUs to APs follow the single-hop star topology, in order to gather the information of WBANs. In this work, we have considered the convergecast model by Zhang *et al.* [30] to collect information from the WBANs. The basic elements of the proposed architecture are defined as follows:

- $\Phi = \{\Phi_1^t, \Phi_2^t, \cdots, \Phi_n^t\}$: Set of criticality indices, where Φ_i^t represents the ctiticality index of the i^{th} WBAN.
- $\mathcal{T} = \{\mathcal{T}_1, \mathcal{T}_2, \cdots, \mathcal{T}_n\}$: Traffic load of each WBAN in a specific area.
- $\psi = \{\psi_1, \psi_2, \cdots, \psi_n\}$: Throughput of each WBAN.
- $\mathcal{P}^t = \{\mathcal{P}_1^t, \mathcal{P}_2^t, \cdots, \mathcal{P}_K^t\}$: Price charged by K number of CSPs at time instant t.
- $\mathcal{G} = \{\mathcal{G}_1, \mathcal{G}_2, \cdots, \mathcal{G}_l\}$: groups formed depending on the relation among coexisting WBANs.
- $d = \{d_1, d_2, \cdots, d_e\}$: e number of disease types present in a particular area.
- $D = \{D_1, D_2, \cdots, D_M\}$: Proximity of the WBANs from Access Points (APs).
- $S_{\mathcal{G}} = \{S_{\mathcal{G}_1}, S_{\mathcal{G}_2}, \cdots, S_{\mathcal{G}_l}\}$: Size of the WBAN groups.

This article has been accepted for publication in a future issue of this journal, but has not been fully edited. Content may change prior to final publication. Citation information: DOI 10.1109/TMC.2018.2822279, IEEE Transactions on Mobile Computing

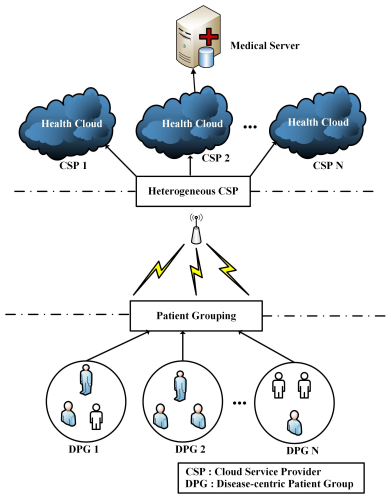

Figure 1: DPG-based Cloud-assisted WBAN Architecture

- $R_{\mathcal{G}}^{d}$: Disease spreading rate in a WBAN group $\mathcal{G}$.
- T and t: Total time duration and a particular time instant, where $T = \{1, 2, \cdots, t\}$.

As depicted in Figure 1, in a emergency situation, the total volume of WBANs in a particular area expendss tremendously, which increases the traffic load of WBANs significantly. In the presence of increased traffic load of cloud-assisted WBANs, the performance of WBANs decrease notably in terms of mapping cost and network throughput. Therefore, to optimize the increased traffic load and maximize the network throughput, WBANs are initiated to form a DPG, depending on distinct syndromes. In the formation of DPG, the WBANs with criticality Φ less than the threshold criticality Φ_{th}, are not included in the same group. For different diseases, the threshold criticality of WBANs differs. After the formation of relation grouping, each group is mapped with a particular CSP. In the traditional WBAN architecture corresponding to a disease, a specific server is dedicated for processing.Therefore, if any disease-specific WBAN is absent in a particular hospital, then the server remains unutilized. However, in a WBAN-cloud if a disease-specific WBAN is absent from a hospital, then that can be used by other disease-based WBANs due to rapid elasticity of the cloud. Therefore, a particular relation based group of WBANs is dedicated to a particular CSP. In the presence of heterogeneous H-CSPs, a specific group-based WBAN selects an optimal H-CSP, depending on the resource available, the total criticality of the WBAN, and the proximity of the AP.

4 Preliminaries

The proposed system uses two approaches — (a) disease-centric relation estimation among WBANs, and (b) cloud computing, for modeling the optimization problem and solution approach, respectively. For easier understanding of the problem formulation, we discuss the basics of the proposed system in this Section. Also, we present the list of symbols used in problem formulation in Table 1.

4.1 Disease-centric Relation Estimation Approach

We elaborate the preliminaries of the disease-centric relation estimation approach for cloud-assisted WBANs.

Definition 1. *DPG is defined as the composition of several WBANs, depending on the distinct syndromes, $d = \{d_1, d_2, \cdots, d_n\}$, where $n \subseteq N$.*

$$\mathcal{G} = \{\hat{n}_1^r, \hat{n}_2^r, \cdots, \hat{n}_t^r\}, \quad (t \subseteq T) \tag{1}$$

where $\hat{n}_t^r$ denotes the average number of WBANs present in a DPG at time t with a relation r.

Definition 2. *Disease-centric relation among WBANs is obtained based on similar disease types, which is calculated using the $n \times n$ encounter matrix. Due to the mobility of WBANs, a WBAN B_i comes in contact with another WBAN B_j. During mutual connection, WBANs transfer its CI Φ and syndromes d with each other using beacon messages. The encounter matrix $n \times n$ is the count of contacts each WBAN encounters. The encounter matrix is defined as,*

$$\mathcal{W}_{i,j} = \begin{cases} 1, & \text{if } B_i \text{ and } B_j \text{ encountered each other} \\ 0, & \text{otherwise} \end{cases} \tag{2}$$

Definition 3. *The disease similarity index (DSI) among WBAN B_i and WBAN B_j is expressed as aff(i, j). Mathematically,*

$$\textit{aff}(i,j) = \begin{cases} 1, & \text{if } d_{B_i} \subseteq d_{B_j} \\ 0, & \text{otherwise} \end{cases} \tag{3}$$

where d_{B_i} and d_{B_j} denote the syndromes of diseases for WBAN B_i and B_j, respectively.

Definition 4. *The relational value r_{ij} denotes the distinct connection Υ among i^{th} WBAN B_i and j^{th} WBAN B_j. The edge is dependent on the type of disease of the concerned patient and the criticality Φ of the WBAN. Mathematically,*

$$r_{ij} = \Upsilon(\Phi_i, \Phi_j) \tag{4}$$

where Φ_t^i and Φ_t^j denotes the criticality indices of i^{th} WBAN and j^{th} WBAN at time t, subsequently.

Definition 5. *Relation matrix $\mathbb{R}$ presents the relation between two WBANs, which is expressed as:*

$$\mathbb{R} = \begin{pmatrix} r_{1,1} & \cdots & r_{1,j} & \cdots & r_{1,n} \\ \vdots & \ddots & \vdots & \ddots & \vdots \\ r_{i,1} & \cdots & r_{i,j} & \cdots & r_{i,n} \\ \vdots & \ddots & \vdots & \ddots & \vdots \\ r_{m,1} & \cdots & r_{m,j} & \cdots & r_{m,n} \end{pmatrix} \tag{5}$$

4.2 Cloud Infrastructure for WBANs

Cloud computing infrastructure supports ubiquitous and elastic resource provision to the real-life applications [31], [32]. Therefore, to store and analyze huge data generated from the

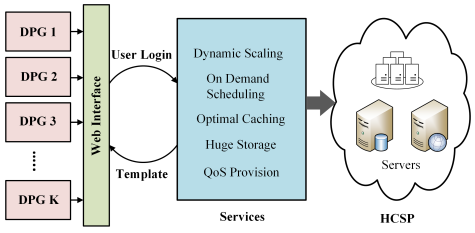

Figure 2: Functionality of Cloud-assisted WBAN Architecture

WBANs, H-CSP provides cost-effective and real-time medical services to the WBANs in a critical emergency situation [33]. Using cloud, it is possible to offer ubiquitous services with elastic demands. In a cloud-assisted WBAN, after sensing the

This article has been accepted for publication in a future issue of this journal, but has not been fully edited. Content may change prior to final publication. Citation information: DOI 10.1109/TMC.2018.2822279, IEEE Transactions on Mobile Computing

physiological data, the body sensors transmit the packets to the health cloud. The health cloud service provider sends the medical data to the medical experts, so that real-time healthcare services can be provision to subscribers.

5 Disease-centric Cluster Formation Among Heterogeneous WBANs

We consider the mobile WBANs in cloud-assisted WBAN architecture. This section theoretically analyzes the necessity of DPG formation for increased traffic load of cloud-assisted WBANs in an area. Whenever the total number of WBANs increases, then the network throughput decreases, and the traffic load in a particular area increases. We discuss the concept of disease-centric cluster formation among WBANs associated with similar disease types, based on SNA [27], to optimize the traffic load and computational complexity of cluster formation. On the other hand, we explain that only DPG formation is not invariably satisfactory for providing QoS-services to WBANs.

5.1 Estimation of Traffic Load

To optimize the traffic load of cloud-assisted WBANs, we need to estimate the effective traffic load, $T^t_{\mathcal{A}}$ of cloud-assisted WBANs in a critical environment in a area $\mathcal{A}$.

Definition 6. *Due to the coexistence of WBANs, the traffic load of a particular WBAN B_i at area $\mathcal{A}$ covered by an AP, A_j, at time t_κ, is calculated as the total number of packets generated $\mathcal{H}_t = \sum_{i=1}^{n} P_i \times t_\kappa$ divided by the covered area [34].*

$$\mathcal{T}_{(P_i,t_\kappa)} = \frac{\sum_{i=1}^{n} P_i \times t_\kappa}{\mathcal{N}(\mathsf{d})} \times \frac{1}{1-p_i} \tag{6}$$

where P_i is the packet transmission rate of WBAN B_i at time t_κ. $\mathcal{H}_t$ denotes the amount of accumulated packets send by these $\mathcal{N}(\mathsf{d})$ number of coexisting WBANs within the area $\mathcal{A}$, d denotes the density of WBANs, and p_i denotes the packet loss rate of WBAN B_i.

Theorem 1. *Increased traffic load in a location decreases the throughput of the WBANs.*

Proof. Let us consider that in a hospital environment a WBAN B_i transmits $\mathcal{K}$ number of successful packets with packet transmission rate P_i at time $t-1$. Then, the throughput is expressed as:

$$\psi_{t-1} = \mathcal{K}\frac{\sum_{i=1}^{n} P_i}{T-1} \times \frac{1}{1-p_i} \tag{7}$$

If the traffic load $t_{(L,t)}$ exceeds the threshold traffic t_{th}, i.e., $(t_{(L,t)} >> t_{th})$ at time t, then the number of successful packets becomes less, as each WBAN wants to send its data, thereby resulting in congestion in the network. Hence, due to channel capacity constraints and potential congestion problems in the network, WBAN B_i transmits h number of successful packets at time t, which is less than the number of successful packets at time $t-1$, i.e., $\mathcal{K} < h$. Therefore, the calculated throughput becomes:

$$\psi_t = h\frac{\sum_{i=1}^{n} P_i}{T} \times \frac{1}{1-p_i} \tag{8}$$

We can observe that the network throughput at time instant t is greater than the network throughput at time $t-1$. Mathematically,

$$\psi_t < \psi_{t-1} \tag{9}$$

Therefore, increased traffic decreases the throughput of WBANs in a particular instant of time. Hence, the proof concludes. □

5.2 Necessity of DPG Formation

Medical emergency situation increases the traffic capacity $\mathcal{T}$ of cloud-assisted WBANs in an area $\mathcal{A}$ covered by an AP, A_k. Therefore, increased traffic load $\mathcal{T}$ in an area $\mathcal{A}$ significantly degrades the performance with respect to mapping cost and service rate. Consequently, due to the resource constrained nature of the AP, an AP is not able to fulfill the bandwidth requirements of all WBANs always and is also not able to provide all the services to the WBANs. In Theorem 2, we prove the necessity of DPG formation.

Theorem 2. *In a hospital environment, under an AP, $\mathcal{N}_{(A,B_i)}$ WBANs get access in an area $\mathcal{A}$. In a medical emergency situation, several new WBANs come into the area A, because of which the criticality index of WBANs increases, $\Phi^i_t << \widehat{\Phi^i_t}$ and associated packet criticality also increases $\Omega^i_t << \widehat{\Omega^i_t}$. Then, the total traffic increases to $\widehat{\mathcal{T}}_{(r,B_i)}$ from $\mathcal{T}_{(r,B_i)}$, i.e., $\widehat{\mathcal{T}}_{(r,B_i)} > \mathcal{T}_{(r,B_i)}$.*

Proof. Suppose, in a medical emergency situation, the total number of WBANs in an area $\mathcal{A}$ covered by an AP, A_j, increases tremendously. The area covered by an AP, A_j, is calculated as:

$$\mathcal{A} = \frac{\pi \mathsf{R}^2 - \mathcal{A}_{\mathsf{R}}}{\sum_{i=1}^{n} \pi a_i^2} \tag{10}$$

where $\pi\mathsf{R}^2$ denotes the total area considered in the proposed model with radius R, $\mathcal{A}_{\mathsf{R}}$ the total area covered by an AP, and $\sum_{i=1}^{n} \pi a_i^2$ the total area covered by WBANs with radius a_i. Therefore, the total traffic load of the WBANs in the area $\mathcal{A}$ is calculated as:

$$\mathcal{T}_{(P_i,t_\kappa)} = \frac{\sum_{\kappa=1}^{\infty}\sum_{i=1}^{n} P_i \times t_\kappa \Omega^i_t}{\frac{(\pi r^2 - A_r)}{\sum_{i=1}^{n} \pi a_i^2} \times g} \times \frac{1}{1-p_i} \tag{11}$$

where p denotes the packet loss per second, d the density of WBANs in the area $\mathcal{A}$, and g the average number of WBANs present in an area. The packet criticality rate Ω^i_t is defined as [35]:

$$\Omega^i_t = f\left(\frac{d^n \varsigma_{\mathcal{B}_i}(t)}{dt^n}, \frac{d^{n-1}\varsigma_{\mathcal{B}_i}(t)}{dt^n}, \cdots, \frac{d\varsigma_{\mathcal{B}_i}(t)}{dt^n}, \varsigma_{\mathcal{B}_i}(t)\right) \tag{12}$$

where $\varsigma_{\mathcal{B}_i}(t)$ denotes the packet generation rate of WBAN $\mathcal{B}_i$. In a critical emergency situation, the number of WBANs increases, i.e, $\mathcal{N}_{tot(A,B_i)} = \mathcal{N}_{(A,B_i)} + \mathcal{N}_{new(A,B_i)}$, where $\mathcal{N}_{new(A,B_i)}$ is the newly arrived WBANs in the area $\mathcal{A}$ covered by an AP. Not only the newly arrived WBANs increase in the area, but also the critcality index $\Phi^i_t << \widehat{\Phi^i_t}$, of WBANs and packet criticality $\Omega^i_t << \widehat{\Omega^i_t}$ increases, with the change in the environment and medical conditions*. Therefore, the total traffic load of the network increases. Mathematically,

$$\widehat{\mathcal{T}}_{(P_i,t_\kappa)} = \frac{\sum_{\kappa=1}^{\infty}\sum_{i=1}^{n} P_i \times t_\kappa \widehat{\Omega^i_t}}{\frac{(\pi r^2 - A_r)}{\sum_{i=1}^{n} \pi a_i^2} \times g} \times \frac{1}{1-p_i} \tag{13}$$

From Equations (11) and (13), we can infer that

$$\widehat{\mathcal{T}}_{(r,B_i)} > \mathcal{T}_{(r,B_i)} \tag{14}$$

As the traffic load increases due to increase in the count of WBANs and their criticality indices, the performance of the total network also degrades. Consequently, the critical WBANs may face medical emergency. Therefore, it is required to decrease the network traffic load, so that each WBAN can get the service optimally. □

*. It depends on the patient's age, sex, height, weight, and location.

This article has been accepted for publication in a future issue of this journal, but has not been fully edited. Content may change prior to final publication. Citation information: DOI 10.1109/TMC.2018.2822279, IEEE Transactions on Mobile Computing

The traffic load of the network increases, due to increase in the number of WBANs and their criticality indices, as stated in Theorem 2. Therefore, the WBANs initiate to form DPG using Algorithm 1. After the formation of DPG, we calculate the individual load of each WBAN. Then, we formulate a network traffic load optimization problem for cloud-assisted WBANs, in order to minimize the increased traffic load, which is expressed as follows:

$$\text{Minimize}\, \mathcal{T}_{(P_i,t_\kappa)} = \left[\frac{\sum_{\kappa=1}^{\infty}\sum_{i=1}^{n} P_i t_\kappa \Phi_t^i}{\frac{(\pi r^2 - A_r)}{\sum_{i=1}^{n} \pi a_i^2} \times g(1-p_i)} \right] \tag{15}$$

$$\text{Subject to} \quad \sum_{i=1}^{n} \mathcal{T}_{(P_i,t_\kappa)} \geq \mathcal{T}_{th}, n \in N \tag{16}$$

$$\Phi_t^i \geq \Phi_t^{th}, t \in \mathcal{T}, n \in N \tag{17}$$

$$P_i \geq P_{th}, i \in n \tag{18}$$

The problem is solved using the Lagrangian Optimization method. We have,

$$\mathcal{L}_{\mathcal{T}} = \frac{1}{\mathcal{T}_{(P_i,t_\kappa)}^{th}} \mathcal{L}_i \left(\frac{\sum_{\kappa=1}^{\infty}\sum_{i=1}^{n} P_i t_\kappa \Phi_t^i}{\frac{(\pi r^2 - A_r)}{\sum_{i=1}^{n} \pi a_i^2} \times g(1-p_i)} \right)$$
$$-\mathcal{X}_1 \left(\sum_{i=1}^{n} \mathcal{T}_{(P_i,t_\kappa)} - \mathcal{T}_{th} \right) - \mathcal{X}_2 \left(\sum_{i=1}^{n}\sum_{t=1}^{T} \Phi_t^i - \Phi_t^{th} \right)$$
$$-\mathcal{X}_3 \left(\sum_{i=1}^{n} P_i - P_{th} \right)$$

where $\mathcal{X}_1$, $\mathcal{X}_2$ and $\mathcal{X}_3$ are the Lagrangian Multipliers constraints. We aim to maximize $\mathcal{T}_{(P_i,t_\kappa)}$ using the approach of Lagrange Multipliers.

Algorithm 1: Algorithm for DPG Formation

Input: Number of WBANs ($B_i \in \mathcal{B}$), criticality index (Φ_t^i), disease similarity index aff(i,j), relational value r_{ij}, waiting time $\tau_{i,t}^*$.
Output: Optimized traffic load $\mathcal{T}_{(P_i,t_\kappa)}^*$

```
Receive information from the present WBANs B_i ∈ B at time t;
Create neighbor list of each WBAN;
Create encounter matrix among WBANs using Equation (2);
Estimate disease similarity matrix using Equation (3);
Find the relation value between two WBANs using Equation (4);
for i = 1 to n do
    if Φ_t^th ≤ Φ_t^i then
        while aff(i,j) == 1 do
            if τ*_{i,t} ≤ δ_th^low then
                Compute τ*_{i,t} = δ_th^low;
                Form Optimal DPG using Equation (1);
                Optimize the traffic load using Equation (15);
            if τ*_{i,t} ≥ δ_th^high then
                Compute τ*_{i,t} = δ_th^high;
                Wait for random amount of time δt;
            Compute τ*_{i,t-1} = τ*_{i,t};
Return T*_{(P_i,t_κ)};
```

5.3 Algorithm for DPG Formation

In this section, we discuss the proposed disease-centric cluster formation algorithm, which takes care of the total traffic of the WBANs in a particular area by forming DPG. Also, it takes care of the energy efficiency of the WBANs. The computational complexity of the DPG algorithm is $O(n)$. We compared the complexity of the proposed scheme with the existing scheme [36], which is relevant to our work. Moulik *et al.* [36] proposed a multi-stage Nash bargaining approach for cost-efficient mapping between WBANs and CSPs. The complexity of this approach is $\mathcal{V}O(n^2)$, where $\mathcal{V}$ denotes the number of stages required for the optimal cost agreement between WBANs and CSPs. Therefore, as the traffic load of WBANs increases, the number of stages required to get the optimal agreement also increases, and inherently, the complexity also increases. Hence, the computational complexity of the DPG algorithm is comparatively lesser than the existing scheme [36].

6 Mapping of DPG to an Optimal H-CSP

Though the process of DPG formation among WBANs decreases the computational complexity and the traffic load of the network, it does not guarantee provisioning of QoS services to each WBAN. Therefore, in this section, we prove that DPG formation is not alone sufficient to provide QoS services to WBANs. To manage QoS services among WBANs, the mapping of DPG to an optimal H-CSP is needed and the selection of critical WBAN from a DPG is also needed. Therefore, the selection of critical WBANs from a DPG is to be decided based on different selection parameters. Consequently, the mapping of DPG to an optimal H-CSP is to be decided based on the pricing model. We consider an architecture of one WBAN B_i and a set of H-CSPs $K = \{1, 2, 3, \cdots k\}$, where K is the total number of H-CSPs. As we consider heterogeneous H-CSPs, we have each H-CSP follow different pricing schemes and accordingly charge different prices to provide the service. The price provided by each H-CSP is denoted as $\mathcal{P} = \{p_1, p_2, \cdots, p_m\}$, where p_m is the maximum price charged by H-CSP. The DPG with group of WBANs is denoted as $G = \{\mathcal{G}_1, \mathcal{G}_2, \cdots \mathcal{G}_{\mathbb{N}}\}$, where $\mathbb{N}$ denotes the total number of DPGs.

6.1 Necessity of Mapping between DPG and Optimal H-CSP

Due to the mobility of WBANs, each WBAN changes its region from one community to another, which significantly changes the QoS and bandwidth requirement of each WBAN. In Theorem 3, we prove the necessity of optimal mapping between a DPG and H-CSP.

Theorem 3. *Due to mobility and underutilization of the local medical server, the conventional WBAN architecture is inefficient. Mapping to an optimal H-CSP provides a Cloud-assisted WBAN more effective health-care services.*

Proof. At time t, the required bandwidth of a WBAN B_i is BW_i^t and the available bandwidth of a local server specific to a disease is BW_L. The total bandwidth requirement of $\mathbb{N}$ number of WBANs within a DPG is expressed as, $BW_{tot}^t = \sum_{i=1}^{\mathbb{N}} BW_i^t$. Due to heavy traffic load $\mathcal{T}$ and mobility of the WBANs, the available bandwidth requirement changes with time. Therefore, the rate of change in bandwidth requirement, Δ_t, at time t is mathematically expressed as:

$$\Delta_t = \frac{\sum_{i=2}^{n} |BW_i^t - BW_i^{t-1}|}{\sum_{t=2}^{T} |t_t - t_{t-1}|} \tag{19}$$

After $t+1$ time, the rate of change in bandwidth requirement of WBANs also increases, as in the presence of different external effects (disease syndrome, environment, and mobility) the criticality index of WBANs increases periodically. On the other hand, if the traffic load traffic load $\mathcal{T}$ increases in an area, then all WBANs do not get fair amount of resources. Therefore, the criticality indices of WBANs with sensitive data increases. The increase in the criticality indices of WBANs also increases the packet generation rate of the body sensor nodes. In such a scenario, the WBANs need increased bandwidth in order to transmit their data packets successfully. Therefore, the rate

This article has been accepted for publication in a future issue of this journal, but has not been fully edited. Content may change prior to final publication. Citation information: DOI 10.1109/TMC.2018.2822279, IEEE Transactions on Mobile Computing

of change in bandwidth requirement, Δ_{t+1}, at time $t+1$ is mathematically expressed as:

$$\Delta_{t+1} = \frac{\sum_{i=2}^{n} |BW_i^{t+1} - BW_i^t|}{\sum_{t=2}^{T} |t_{t+1} - t_t|} \tag{20}$$

Due to the variation in the criticality indices of WBANs, the rate of change in the bandwidth requirement at time $t+1$ increases over the rate of change in bandwidth requirement at time t, $(\Delta_{t+1} >> \Delta_t)^{\dagger}$. This is because the rate of change in bandwidth requirement varies with time and criticality index. Therefore, the available bandwidth, BW_L, on a local server is not enough to fulfill its requirements. Mathematically,

$$BW_L < \Delta_{t+1} \sum_{i=1}^{\mathbb{N}} BW_i^t << \Delta_{t+1} \sum_{i=1}^{\mathbb{N}} BW_i^{t+1} \tag{21}$$

As the available bandwidth does not fulfill the required bandwidth, there is a requirement of optimal mapping between WBANs and CSPs, in order to provide fair resources among WBANs with optimal price. However, the bandwidth requirement converges at a point, when the the bandwidth requirement reaches the maximum bandwidth availability of a local server BW_L^{max}. Mathematically,

$$BW_L < \Delta_{t+1} \sum_{i=1}^{\mathbb{N}} BW_i^t << \Delta_{t+1} \sum_{i=1}^{\mathbb{N}} BW_i^{t+1} \geq BW_L^{max} \tag{22}$$

Hence, the proof concludes. □

Remark 1. *In the absence of a particular disease, d_i, the affected WBANs in a hospital make the particular disease-centric server unutilized and inefficient.*

Suppose, the capacity of a local server corresponding to a particular disease d_i in a hospital be $\mathbb{C}_{d_i}$. The utilization factor of the local server $\mathbb{S}_i$ is mathematically expresses as, $\mathbb{U}_{\mathbb{S}_i} = \frac{\mathbb{C}_{d_i}}{\beta}$. Here, β is the arrival rate of the WBANs of a particular disease type. If the present arrival rate $\bar{\beta}$ of WBANs specific to a disease type decreases, then the revised utilization factor decreases. Mathematically,

$$\bar{\mathbb{U}}_{\mathbb{S}_i} < \mathbb{U}_{\mathbb{S}_i} \tag{23}$$

Hence, in the absence of a particular disease d_i, the affected WBANs in a hospital make the particular disease-centric server unutilized and inefficient.

6.2 Selection Parameters

After the formation of different DPGs, we need to identify the critical WBANs from each DPG to optimize the traffic capacity of cloud-assisted WBANs. The election of critical WBANs is to be decided depending on different election parameters. They are discussed below.

- **Criticality Index of WBAN**: The *criticality index* of a WBAN B_i at time t is denoted by Φ_i^t [37], and is presented as:

$$\Phi_i^t = \left| \frac{(\ominus_{uc} - \ominus_t)^2 - (\ominus_t - \ominus_{lc})^2}{(\mid \ominus_{uc} \mid + \mid \ominus_{lc} \mid)^2} \right| \tag{24}$$

where $\ominus_{uc}$ and $\ominus_{lc}$ are the upper and lower range of a physiological specification of a patient. $\ominus_t = \frac{(\ominus_{uc} + \ominus_{lc})}{2}$ defines the measurement of distinct physiological data.

- **Proximity to AP**: The utility of the H-CSP $\mathcal{U}_{S_j}^{\mathcal{G}_i}(t)$ depends on the distance between the WBAN $B_i^{\mathcal{G}_k}$ in the group G_k.

$$D_{(B_i,AP)} = \left(1/\sqrt{(B_i^x - AP_j^x)^2 + (B_i^y - AP_j^y)^2} \right) \tag{25}$$

where (B_i^x, B_i^y) and (AP_j^x, AP_j^y) are the coordinates of i^{th} WBAN and j^{th} AP, respectively.

- **Size of DPG**: Size of the j^{th} relational group is presented as $S_{\mathcal{G}_i}^t$ at time t. Mathematically,

$$\sum_{j=1}^{\mathbb{N}} S_{\mathcal{G}_j}^t = \sum_{j=1}^{\mathbb{N}} \tilde{N}^{\mathcal{G}_j} \quad , \quad 1 \leq j < \mathbb{N} \tag{26}$$

where $\tilde{N}^{\mathcal{G}_j}$ denotes the number of WBANs present in a group $\mathcal{G}_j$, based on the disease based relation r.

- **Epidemic Spread Factor (ESF)**: Epidemic spread factor denotes the change or the deviation in the criticality index Φ_t of the WBANs in a particular group $\mathcal{G}_j$, and is denoted by Υ.

$$\Upsilon = \Phi_{i,\mathcal{G}_j}^t - \Phi_{i,\mathcal{G}_j}^{t-1} \tag{27}$$

where $\Phi_{i,\mathcal{G}_j}^t$ and $\Phi_{i,\mathcal{G}_j}^{t-1}$ are criticalities of the WBAN refer to a particular group at a time t and $t-1$ respectively.

- **Residual Energy Level**: The residual energy level of WBANs is presented as $\Psi_{B_i}^t$, and is mathematically expressed as, $\Psi_i^t = \frac{E_i^{pre}}{E_i^{ini}}$. Here, E_i^{pre} and E_i^{ini} denote the required and preliminary energy levels of the i^{th} WBAN B_i, subsequently.

- **Available Bandwidth of the H-CSP**: Available bandwidth of the H-CSP is calculated as,

$$BW_{ava} = BW_{tot} - BW_{use} \tag{28}$$

where BW_{tot} and BW_{use} denote the total and used bandwidths of the H-CSP, respectively.

Definition 7. *The utility factor $\mathcal{S}_i^{\mathcal{G}_j}$ of a WBAN, B_i, affinity to a group, $\mathcal{G}_j$, to choose an H-CSP among heterogeneous H-CSPs at time t, is expressed as,*

$$\mathcal{S}_i^{\mathcal{G}_j} = \mu \left(\frac{E_i^{pre}}{E_i^{ini}} + S_{\mathcal{G}_j}^t \frac{|\Phi_{i,\mathcal{G}_j}^t - \Phi_{i,\mathcal{G}_j}^{t-1}|}{\Phi_t} + \frac{D_{(B_i,AP)^{min}}}{D_{(B_i,AP)^{max}}} + \frac{BW_{ava}}{BW_{tot}} \right) \tag{29}$$

where μ denotes utility constant, Φ_t denotes criticality index and ψ denotes epidemic spreading factor. $D(B_i, AP)^{max}$ and $D(B_i, AP)^{min}$ denote maximum and minimum the distance between a WBAN and an AP, respectively.

The utility constant, μ, of the utility factor is expressed as,

$$\mu = \begin{cases} 1, & \text{if } E_{B_i}^{ini} \leq E_{B_i}^{pre} \\ 0, & \text{otherwise} \end{cases} \tag{30}$$

The maximization of the selection rate $\mathcal{S}_i^{\mathcal{G}_j}$ is defined as follows:

$$\vartheta = \text{Max} \;\; \mathcal{S}_i^{\mathcal{G}_j}, \; \forall i \in n, \mathcal{G} \in G \tag{31}$$

Theorem 4. *The maximum and minimum values of the selection parameter is expressed as:*

$$f_{(\mathcal{S}_i^{\mathcal{G}_j})}^{max} = \left(2 + \frac{0.5\mathbb{Y}}{\mathcal{F}} \right) \tag{32}$$

$$f_{(\mathcal{S}_i^{\mathcal{G}_j})}^{min} = \left(1 + 0.5\bar{\mathbb{Y}} + \frac{1}{\bar{\beta}} \right) \tag{33}$$

†. However, this conclusion is only true, if the traffic load of WBANs in an area exceeds the predefined threshold limit.

This article has been accepted for publication in a future issue of this journal, but has not been fully edited. Content may change prior to final publication. Citation information: DOI 10.1109/TMC.2018.2822279, IEEE Transactions on Mobile Computing

Proof. The selection function, f_i, is a linear function of variables RE, D, and BW, and Θ is a constant for choosing the critical WBANs. The function is derived by subtracting the cost function from the selection rate function shown in Equation (29). The selection rate in Equation (29) gives the maximum value. The selection rate is maximum when $E_i^{pre} = E_i^{ini}$ and $D_{(B_i,AP)^{min}} = D_{(B_i,AP)^{max}}$. Therefore the maximum selection rate is expressed as:

$$f_{(\mathcal{S}_i^{\mathcal{G}_j})}^{max} = \left(2 + \frac{0.5\mathbb{Y}}{\mathcal{F}}\right) \tag{34}$$

where $\mathbb{Y}$ is the maximum size of the DPG and $\frac{0.5}{\mathcal{F}}$ is the maximum criticality index, $\mathcal{F} < 1$. Also,

$$\frac{E_{B_i}^{pre}}{E_{B_i}^{ini}} + \frac{D_{(B_i,AP)_{min}}}{D_{(B_i,AP)_{max}}} = 2 \tag{35}$$

The selection rate is minimum when $\frac{1}{\beta} < \frac{E_{B_i}^{pre}}{E_{B_i}^{ini}}$ and the minimum size of the DPG is $\bar{\mathbb{Y}}$. The minimum selection rate is expressed as:

$$f_{(\mathcal{S}_i^{\mathcal{G}_j})}^{min} = \left(1 + 0.5\bar{\mathbb{Y}} + \frac{1}{\bar{\beta}}\right)$$

therefore, we get the maximum and minimum values of the selection parameter. Hence the proof concludes. □

Lemma 1. *Every critical WBAN has its own preference of choosing optimal H-CSP. Therefore, the preference P_i of the WBAN B_i of choosing H-CSP C_i among heterogeneous H-CSPs are the symmetric and asymmetric components of the relation.*

Proof. Suppose, the WBAN $B_i^{\mathcal{G}_h}$ belongs to group $\mathcal{G}_h$ with relation r_h having a preference of choosing H-CSP S_m and another WBAN $B_j^{\mathcal{G}_h}$ belongs to group $\mathcal{G}_k S$ with relation r_k having a preference of choosing H-CSP S_n. As the WBANs belong to the different groups $\mathcal{G}_h$ and $\mathcal{G}_k$, each WBAN from the different groups has the different preferences P_p and P_o of choosing H-CSP. Then, the WBANs follow asymmetricity, which is expressed as,

$$B_i^{\mathcal{G}_h} r_h S_m P_p \not\Rightarrow B_j^{\mathcal{G}_k} r_k S_n P_o \tag{36}$$

For the asymmetricity statement, it is assumed that the relations among WBANs are different. It is also assumed that they belong to different groups. Therefore, the WBANs do not know one another's preferences of choosing optimal H-CSP. For the mapping process, WBANs take a cumulative decision in order to get an optimal solution between WBANs and CSPs, based on one another's individual preferences. As the WBANs belong to different groups, they cannot take any cumulative decision to choose an optimal decision. Consequently, we designed our scheme in such a way that the WBANs belonging to different groups and relations must follow an asymmetric relation. Suppose, the WBAN $B_i^{\mathcal{G}_h}$ and another WBAN $B_j^{\mathcal{G}_h}$ belong to the same group $\mathcal{G}_h$ with relation r_k having a preference P_p of choosing H-CSP S_m. As the WBAN B_i and B_j belong to the same group $\mathcal{G}_h$, all the WBANs in the group have the same preference of choosing P_p the H-CSP. Then, the WBAN follows symmetricity, which is expressed as,

$$B_i^{\mathcal{G}_h} P_p S_m r_k \Rightarrow B_j^{\mathcal{G}_h} P_p S_m r_k \tag{37}$$

Similarly, for the symmetricity statement, the relation among WBANs are the same, and also they belong to the same group. Therefore, the WBANs know the preferences of one another for choosing the optimal H-CSP. For the mapping process, WBANs take a cumulative decision in order to get an optimal between the WBANs and the CSPs, based on the individual preferences. As the WBANs belong to the same group, they can take the cumulative decision to choose an optimal CSP. With this objective, we designed our scheme in a manner that the WBANs belonging to the same group and relation must follow a symmetric relation. Hence, the proof concludes. □

6.3 Formulation of Utility Function

The WBAN $B_i^{\mathcal{G}_j}$ belonging to group $\mathcal{G}_j$ can be model as a customer and expecting to obtain more benefits with least possible payments. The utility function of WBAN is expressed as,

$$\mathcal{U}_{B_i^{\mathcal{G}_j}} = \mathcal{R}_{B_i} - \mathcal{P}_{tot} \tag{38}$$

where $\mathcal{R}(.)$ defines the revenue function and $P(.)$ denotes the price charged by the H-CSP or total charge payed by the WBAN. The revenue function $\mathcal{R}(.)$ defines the selection rate of choosing a H-CSP $\mathcal{S}_i^{\mathcal{G}_j}$. It is mathematically expressed as,

$$\mathcal{R}_{B_i} = \eta \times \sum_{j=1}^{\mathbb{N}} \mathcal{S}_i^{\mathcal{G}_j} \tag{39}$$

where η denotes the gain per unit selection rate. $P(.)$ defines the total charge payed by the WBAN for using cloud services. It is mathematically expressed as follows:

$$\mathcal{P}_{tot} = \sum_{i=1}^{n} \mathcal{P}_i^t \times \mathcal{R}_{C_k} + \mathcal{P}_{QoS} \tag{40}$$

where $\mathcal{P}_i^t$ represents the price per unit of resource selling from H-CSP C_k to WBAN, $\mathcal{R}_{C_k}$ represents the amount of resource bought by WBAN from H-CSP, and $\mathcal{P}_{QoS}$ represents the fixed price charged by all the H-CSPs to give QoS to the WBAN.

We segregated the QoS satisfying pricing into two categories, as follows:

a) Price charged for interference management among coexisting WBANs in an area, $\mathcal{A}$, is denoted as, $\mathcal{P}_I$. Therefore, the interference management factor is expressed as:

$$\alpha_{k,l} = \sum_{k=1}^{K} \beta(I) a_{k,l} \tag{41}$$

where $\beta(I)$ denotes the interference management factor and $a_{k,l}$ denotes the price charged by the H-CSP to manage the interference among the coexisting WBANs. The price charged per WBAN for interference management, $\mathcal{P}_I$, is expressed as:

$$\mathcal{P}_I = \sum_{i=1}^{n} \left(\frac{\sum_{l=1}^{\bar{M}} \alpha_{k,l}}{M_i} \right) \tag{42}$$

where M_i denotes the average number of coexisting WBANs and $\bar{M}$ denotes the total number of coexisting WBANs in an area. Hence, the total price charged per WBAN by H-CSP for interference management is expressed as:

$$\mathcal{P}_I = \sum_{i=1}^{n} \frac{1}{M_i} \left\{ \sum_{l=1}^{\bar{M}} \sum_{k=1}^{K} \beta(I) a_{k,l} \right\} \tag{43}$$

b) Price charged for queue and mobility management, is denoted as $\mathcal{P}_Q$. Therefore, the queue and mobility man-

This article has been accepted for publication in a future issue of this journal, but has not been fully edited. Content may change prior to final publication. Citation information: DOI 10.1109/TMC.2018.2822279, IEEE Transactions on Mobile Computing

agement factor is expressed as:

$$\Lambda_{k,l} = \bar{\Lambda} \sum_{i=1}^{n} \varpi_i(\mathcal{I}) + \mathcal{Q}_i \tag{44}$$

where $\bar{\Lambda}$ denotes the price charged by H-CSP to manage the problem related to queue overflow and transient connection due to mobility. $\varpi_i(\mathcal{I})$ and $\mathcal{Q}_i$ denote the mobility and queue management factor for WBAN B_i. The queue and mobility management price charged from WBAN is expressed as:

$$\mathcal{P}_Q = \sum_{i=1}^{n} \sum_{k=1}^{K} \left\{ \frac{V_{max}(\sum_{l=1}^{\bar{M}} \Lambda_{k,l})}{V_i^{t_1} + V_i^{t_2} + \cdots + V_i^{t_t}} \right\} \tag{45}$$

where V_{max} denotes the maximum velocity of a WBAN and V_i^1 denotes the velocity of WBAN B_i at different time instant.

Therefore, the total price charged by H-CSP for QoS management of WBANs, P_{QoS}, is expressed as:

$$\mathcal{P}_{QoS} = \mathcal{P}_I + \mathcal{P}_Q \tag{46}$$

$$\mathcal{P}_{QoS} = \sum_{i=1}^{n} \left[\frac{1}{M_i} \sum_{l=1}^{\bar{M}} \sum_{k=1}^{K} \beta(I) a_{k,l} + \frac{V_{max} \sum_{k=1}^{K} (\sum_{l=1}^{\bar{M}} \Lambda_{k,l})}{V_i^{t_1} + V_i^{t_2} + \cdots + V_i^{t_t}} \right] \tag{47}$$

The optimization problem for optimal mapping between WABNs and CSPs is mathematically expressed as:

$$\text{Maximize} \quad \sum_{i \in n, j \in \mathbb{N}} \mathcal{U}_{B_i^{\mathcal{G}_j}} = \left[\eta \times \sum_{j=1}^{\mathcal{N}} \mathcal{S}_i^{\mathcal{G}_j} - \mathcal{P}_{tot} \right] \tag{48}$$

$$\text{Subject to} \quad \sum_{i=1}^{n} \sum_{i=1}^{\mathbb{N}} \mathcal{S}_i^{\mathcal{G}_j} \geq \sum_{i=1}^{n} \mathcal{S}_i^{th}, n \in N \tag{49}$$

$$\Phi_t^i \geq \Phi_t^{th}, t \in \mathcal{T}, n \in N \tag{50}$$

$$\mathcal{P}_{tot} \geq \mathcal{P}_{th}) \tag{51}$$

Therefore, the characteristic of the utility function is expressed as follows:

i) The first order derivative of the utility function is a non-decreasing function, as each WBAN attempts to map with the optimal H-CSP in a cost effective way. Mathematically, we have:

$$\frac{\partial \mathcal{U}_{B_i^{\mathcal{G}_j}}}{\partial t} \geq 0 \tag{52}$$

ii) The second order derivative of the utility function is decreasing function, so that each WBAN gets the maximum utility value. Mathematically we have:

$$\frac{\partial^2 \mathcal{U}_{B_i^{\mathcal{G}_j}}}{\partial t^2} \leq 0 \tag{53}$$

As the WBAN $B_i^{\mathcal{G}}$ in the group $\mathcal{G}_j$ tries to maximize the utility $\mathcal{U}_{B_i^{\mathcal{G}_j}}$ by buying optimal amount of resources, the utility $\mathcal{U}_{B_i^{\mathcal{G}_j}}$ varies with the resource for a WBAN $B_i^{\mathcal{G}}$.

$$\left(\frac{\partial \mathcal{U}_{B_i^{\mathcal{G}_j}}}{\partial t} = \eta \times \frac{\partial \mathcal{S}_i^{\mathcal{G}_j}}{\partial t} - \sum_{i=1}^{n} \mathcal{P}_i^t \times \mathcal{R}_{C_k} - \mathcal{P}_{QoS} \right) \tag{54}$$

If $\mathcal{P}_i^t \leq \frac{\partial \mathcal{S}_i^{\mathcal{G}_j}}{\partial t}$, then from Equation (54), we can conclude,

$$\frac{\partial \mathcal{U}_{B_i^{\mathcal{G}_j}}}{\partial t} > 0 \tag{55}$$

Theorem 5. *Though the size of the relational group does matter, but the provision to the H-CSP mainly depends on the disease spreading factor of a particular group.*

Proof. Suppose, in the proposed architecture, the size of the H-CSP is classified into Small-cloud ($S_{\mathcal{G}^s}$), Medium-cloud ($S_{\mathcal{G}^m}$) and Large-cloud ($S_{\mathcal{G}^l}$), depending upon their computational power (P_{com}) and the resource poll (i.e., bandwidth BW, and the access time T_{acc}).

Let, the disease spread factor of the i^{th} group be $\psi_{\mathcal{G}_i}$. Therefore, the disease spread factor of different groups is denoted as $\Upsilon = \{\Upsilon_{\mathcal{G}_1}, \Upsilon_{\mathcal{G}_2}, \Upsilon_{\mathcal{G}_3}, \cdots, \Upsilon_{\mathcal{G}_l}\}$. Based on this, each group is assigned a different cloud. Let $\Upsilon_{\mathcal{G}_1}$, $\Upsilon_{\mathcal{G}_2}$ and $\Upsilon_{\mathcal{G}_3}$ be the disease spread factor of the groups $\mathcal{G}_1$, $\mathcal{G}_2$ and $\mathcal{G}_3$. At a specific time t, the disease spread factor of $\mathcal{G}_1$ is higher than the same for $\mathcal{G}_2$, and the disease spread factor of the $\mathcal{G}_2$ is higher than the same for $\mathcal{G}_3$. This is mathematically expressed as,

$$\Upsilon_{\mathcal{G}_1} > \Upsilon_{\mathcal{G}_2} > \Upsilon_{\mathcal{G}_3} \tag{56}$$

Similarly, at time t, the size of the group $\mathcal{G}_1$ is higher than the same for $\mathcal{G}_2$, and the size of the group of the $\mathcal{G}_2$ is higher than the same for $\mathcal{G}_3$. Mathematically,

$$\mathcal{G}_1 > \mathcal{G}_2 > \mathcal{G}_3 \tag{57}$$

However, we use the incentive compatibility mechanism [38] in order to prove the Theorem. Let, a WBAN with the disease spreading factor, $\Upsilon_{\mathcal{G}_i}$, of a $\mathcal{G}_i$ be mapped to the small-cloud $S_{\mathcal{G}^s}$. However, if the disease spreading factor, $\Upsilon_{\mathcal{G}_i}$ of that group is greater than the threshold disease spreading factor, Υ_{th}, i.e., $\Upsilon_{\mathcal{G}_i} >> \Upsilon_{th}$, then the WBANs with the increased spreading factor in that particular group do not get fair resources from $S_{\mathcal{G}^s}$. In such a condition, the incentive compatibility constraint ensures that, instead of mapping the WABNs to $S_{\mathcal{G}^s}$, the WBANs are mapped to the medium-cloud $S_{\mathcal{G}^m}$ for efficient utilization of the resources. Mathematically,

$$\Upsilon_{\mathcal{G}_i} >> \Upsilon_{th}, S_{\mathcal{G}^m} > S_{\mathcal{G}^s} \tag{58}$$

Similarly, a WBAN with disease spreading factor, $\Upsilon_{\mathcal{G}_i}$, of a $\mathcal{G}_i$ is mapped to the medium-cloud $S_{\mathcal{G}^m}$. However, if $\Upsilon_{\mathcal{G}_i}$ of that group is greater than the threshold disease spreading factor, Υ_{th}, i.e., $\Upsilon_{\mathcal{G}_i} >> \Upsilon_{th}$, then the WBANs with the increased disease spreading factor in that particular group do not get fair resources from $S_{\mathcal{G}^m}$. In such condition, the incentive compatibility constraint ensures that instead of mapping the WABNs to $S_{\mathcal{G}^m}$, the WBANs are mapped to the large-cloud $S_{\mathcal{G}^l}$ for efficient utilization of the resources. Mathematically,

$$\Upsilon_{\mathcal{G}_i} >> \Upsilon_{th}, S_{\mathcal{G}^l} > S_{\mathcal{G}^m} \tag{59}$$

In such a scenario, at the same time t, $\mathcal{G}_1$ is assigned to the Large-cloud ($S_{\mathcal{G}^l}$). As the size of the group is large and also the disease spreading factor increases with time, therefore $\mathcal{G}_1$ can not mapped with $S_{\mathcal{G}^s}$ and $S_{\mathcal{G}^m}$. It is mathematically expressed as:

$$(\mathcal{G}_1 \rightarrow S_{\mathcal{G}^l}) \text{ at access time } (T_{acc}) \tag{60}$$

Also, $\mathcal{G}_2$ is assigned to the Medium-cloud ($S_{\mathcal{G}^l}$). Mathematically, it is expressed as,

$$(\mathcal{G}_2 \rightarrow S_{\mathcal{G}^m}) \text{ at access time } (T_{acc}) \tag{61}$$

Also, $\mathcal{G}_3$ is assigned to the Small-cloud ($S_{\mathcal{G}^l}$). Mathematically, it is expressed as,

$$(\mathcal{G}_3 \rightarrow S_{\mathcal{G}^s}) \text{ at access time } (T_{acc}) \tag{62}$$

Therefore, based on the disease spread factors different H-CSPs

This article has been accepted for publication in a future issue of this journal, but has not been fully edited. Content may change prior to final publication. Citation information: DOI 10.1109/TMC.2018.2822279, IEEE Transactions on Mobile Computing

are provided using the incentive compatibility mechanism. Hence, the proof concludes. □

The total number of requested WBANs belonging from a group $\mathcal{G}$ is denoted by $\Re$. We get,

$$\Re = \sum_{i=1}^{n} \mathcal{Z}_i^{\mathcal{G}} \tag{63}$$

where $\mathcal{Z}_i^{\mathcal{G}}$ represents the request of the i^{th} WBAN in a particular group $\mathcal{G}$. Therefore, within a particular group $\mathcal{G}$ total $\Re$ number of requests are sent by WBANs belonging to the same group. If the WBAN requests are satisfied by the H-CSPs at time t, then the satisfaction factor for each WBAN is denoted by Π_{B_i}. It is mathematically expressed as,

$$\Pi_{B_i} = \left[\frac{\left(\sum_{i=1}^{n} \sum_{j=1}^{\mathbb{N}} t - \hat{t} \right) \times \mathcal{U}_{B_i^{\mathcal{G}_j}}}{\sum_{i=1}^{n} \mathcal{Z}_i^{\mathcal{G}}} \right] \tag{64}$$

Using the Lagrange multiplier, we express the optimization problem in Equation (51) as,

$$\bigtriangledown_{i \in n} \mathcal{U}_{B_i^{\mathcal{G}_j}} = -\lambda \bigtriangledown_{i \in n} \mathcal{U}_{B_i^{\mathcal{G}_j}} \tag{65}$$

$$\left[\frac{\delta \mathcal{U}_{B_i^{\mathcal{G}_j}}}{\delta t_1}, \frac{\delta \mathcal{U}_{B_i^{\mathcal{G}_h}}}{\delta t_2}, \cdots, \frac{\delta \mathcal{U}_{B_i^{\mathcal{G}_j}}}{\delta t_t} \right] \begin{bmatrix} \lambda_{t_1} \\ \lambda_{t_2} \\ \vdots \\ \lambda_{t_t} \end{bmatrix} = 0 \tag{66}$$

$$\text{where,} \quad \bigtriangledown_{i \in n} \mathcal{U}_{B_i^{\mathcal{G}_j}} = \left(\frac{\partial \delta \mathcal{U}_{B_i^{\mathcal{G}_j}}}{\partial t}, \frac{\partial \delta \mathcal{U}_{B_i^{\mathcal{G}_j}}}{\partial \bar{t}} \right) \tag{67}$$

6.4 Algorithm for Mapping to an Optimal H-CSP

In this section, we propose an algorithm to choose an optimal H-CSP among heterogeneous H-CSPs in a medical emergency situation. From Algorithm 1, we get the WBANs with the similar disease types in a DPG to choose the critical ones within the cluster easily and achieve lower computational complexity. Algorithm 2 describes the mapping of DPG to an optimal H-CSP, to provide fair amount of resources to the critical WBANs in a medical emergency situation.

7 Complexity Analysis

In Section, we analyze the performance of the proposed scheme theoretically. We discuss the complexity of the proposed scheme for cloud-assisted WBANs.

Theorem 6. *The worst case asymptotic time complexity of the system is $O(zn^2)$, where n is the number of critical WBANs.*

Proof. In the first algorithm, each WBAN related to the same disease forms a cluster to minimize the computational complexity. To form the DPG, the worst case computation complexity is $O(qn)$ from Algorithm 1. After the formation of DPG, the critical WBANs choose from the DPG. To choose the critical WBANs from each WBAN, a selection procedure using the selection parameter $\mathcal{S}_i$. Therefore, the worst case complexity of selecting critical WBANs is $O(pn)$.

$$\mathbb{T}(X) = \mathbb{C}_1\{q\mathbb{T}(X_s) + p\mathbb{T}(X_k)\} + \mathbb{C}_2\mathbb{T}(1) \tag{68}$$

The combined worst case complexity of DPG formation and selection of critical WBANs is $O(zn^2)$, where $z = q + p$. Hence, we infer that the total computational complexity of the proposed approach, in the worst case, is $O(zn^2)$, where n is the count of critical WBANs. This completes the proof. □

Algorithm 2: Algorithm for Mapping to Optimal H-CSP

Input: Number of WBANs within a DPG ($B_i \in \mathcal{B}$), Disease types $d = \{d_1, d_2, \cdots, d_k\}$, Ctiticality index of each WBAN Φ_t^i, waiting time $\tau_{i,t}^*$.
Output: Optimal Mapping Matrix ($\mathcal{U}^*_{B_i^{\mathcal{G}_j}}$)

```
Calculate the criticality index of all WBANs B_i ∈ B at time t;
Measure the Euclidean distance between WBAN and the gateway ;
Compute the group size of the DPG, S^t_{G_i};
Compute the disease spread factor within the DPG;
Calculate the residual energy level of the each WBAN;
Compute the available bandwidth for the AP;
Compute the selection parameter S_i, ∀B_i ∈ B;
if S^{G_i}_{S_j} ≥ S^{th}_{S_j} then
    The detected WBANs are in critical medical condition in a DPG;
    Update waiting time τ*_{i,t} = δ^{low}_{th};
    if U_{B_i^{G_h}} ≥ U^{th}_{B_i^{G_h}} then
        Optimal Mapping matrix U*_{B_i^{G_j}};
        QoS is provided by the H-CSP with extra price P_{QoS};
    if U_{B_i^{G_h}} ≤ U^{th}_{B_i^{G_h}} then
        Standard mapping matrix generated;
        QoS is not provided by the H-CSP;
if S_i^{G_j} ≤ S_i^{th} then
    The detected WBANs are in normal medical condition in a DPG;
    Update waiting time τ*_{i,t} = δ^{high}_{th};
Update τ*_{i,t-1} = τ*_{i,t};
Return U*_{B_i^{G_j}};
```

Table 1: Testbed Information

Parameters	Values
Processor Used	Intel(R) i5-2500 CPU @ 3.30 GHz
RAM	4GB, DDR3
Disk Space	320 GB
Operating System	Ubuntu 14.04 LTS
Application Software	MATLAB R2013a

8 Performance Evaluation

We discuss the results of the proposed schemes, based on different metrics. We have used a modeled and created simulation platform using MATLAB. We have given the system information in Table 1 and also enlisted the simulation parameters in Table 2.

Table 2: Simulation Parameters

Parameter	Value
Simulation area	1 $Km \times$ 1 Km
Number of WBANs	300
Number of body sensors in a WBAN	8
Number of APs	10
Velocity of each WBAN	1.5 m/s
Initial energy WBAN	0.5 J
Power consumption of Tx-circuit	16.7 nJ
Power consumption of Rx-circuit	36.1 nJ
Power consumption of Amplifier-circuit	1.97 nJ
Energy of WBANs	0.5 J
SINR threshold	5-15 dB
Sensing range of body sensors	$0.5 - 1.5$ m
Packet rate	4 packets/sec
Packet size	512 Bytes

8.1 Benchmarks

CHMS, the benchmark considered in this study, is a cloud-based medical system, proposed by Almashaqbeh *et al.*, [39]. The authors proposed a data aggregation and classification system to reduce the traffic load of the network. They also proposed a dynamic channel assignment approach to reduce the interference among coexisting WBANs. As the benchmark

This article has been accepted for publication in a future issue of this journal, but has not been fully edited. Content may change prior to final publication. Citation information: DOI 10.1109/TMC.2018.2822279, IEEE Transactions on Mobile Computing

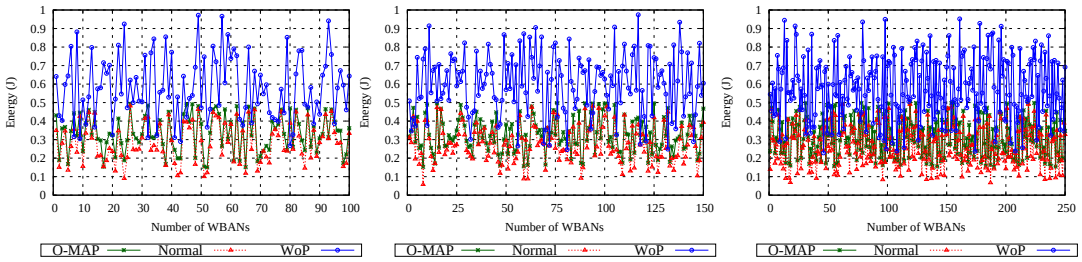

(a) 100 WBANs, 5 H-CSPs (b) 150 WBANs, 10 H-CSPs (c) 200 WBANs, 15 H-CSPs

Figure 3: Fixed Number of WBANs with Varying Number of H-CSPs

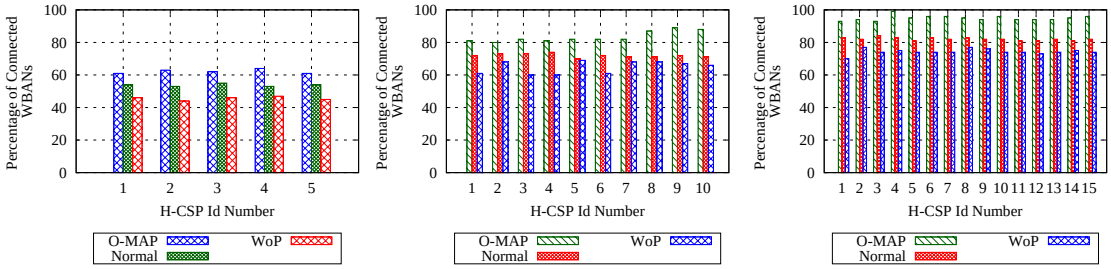

(a) Number of H-CSP, 5 (b) Number of H-CSP, 10 (c) Number of H-CSP, 15

Figure 4: Fixed Number of WBANs with Varying Number of H-CSPs

algorithm proposed a traffic flow based dynamic channel assignment approach for cloud-assisted WBANs, therefore we have considered this approach to compare it with our existing scheme.

8.2 Simulation Settings

To analyze the performance of the two schemes — Efficient Healthcare Management (HCM) and Optimal Mapping (O-MAP), we considered the Group-based mobility of WBANs [40]. Also, we considered the single-hop star topology for data transmission in WBANs, where each WBAN consists of 8 sensor nodes placed on the body, according to [41]–[43]. The WBANs are distributed randomly in an area of 1 $Km\times$ 1 Km. To consider the varying traffic of WBANs in an area, we vary the WBAN density factor g from 5 to 20 per square meter. Also, we vary the traffic load from 500 Kbps to 950 Kbps to observe the mapping cost between WBANs and H-CSPs. Subsequently, we considered the different data rates of body senor nodes, i.e., 100 Kbps to 700 Kbps, to compute the optimal mapping cost of WBANs. For the validation of our proposed approach, we use the IEEE 802.15.4 standard CSMA/CA access mechanism [44]. The price function for mapping is defined as $f(\mathcal{P}_{tot}) = \mathcal{P}^t_Q(y^t_{b_i})^2$, where $y^t_{b_i}$ defines the data transmission rate of the sensor nodes.

8.3 Performance Metrics

We illustrate the different performance metrics used for performance evaluation.

- *Network Throughput*: Network throughput is defined as the number of packets successfully received per second.
- *Traffic Load*: Traffic capacity of the network defines the total number of packets transmitted from a DPG per second.
- *Residual Energy*: Residual energy of a WBAN defines the initial energy of the WBAN to perform different operations.
- *Packet Delivery Delay*: Packet delivery delay defines the time duration between the data transmitted from the WBAN to the data received at the AP.
- *Packet Loss*: Packet loss defines the difference between the number of data packets transmitted from the WBAN to the total amount of data packets received at the AP per unit time.

$$\sigma = \frac{\mathbb{P}^t_{tran} - \mathbb{P}^t_{rec}}{t} \tag{69}$$

where $\mathbb{P}^t_{tran}$ and $\mathbb{P}^t_{rec}$ denote the amount of data packets transmitted and the number of packets received at time t, respectively.

- *Service Rate*: Service rate denotes the ratio of the number of patients served to the number of patients present in the area.

$$\mathbb{S} = \frac{\mathcal{N}^t_{ser}}{\mathcal{N}^t_{tot}} \tag{70}$$

where $\mathcal{N}^t_{ser}$ and $\mathcal{N}^t_{tot}$ present the amount of patients served and the total amount of patients at time t, respectively.

- *Average Energy Consumption*: Energy consumption of each WBAN, $\mathbb{E}$, is calculated as [45]:

$$\mathbb{E}_i = \mathbb{E}_0 - \mathbb{K}(\mathbb{E}_{elec} + \epsilon_{amp})\mathcal{D}^2 \tag{71}$$

where $\mathbb{E}_0$ denotes the initial energy, $\mathbb{E}_{elec}$ the energy consumption due to electric circuit and ϵ_{amp} the energy consumption due to amplifier circuit. $\mathbb{K}$ denotes the packet size and $\mathcal{D}$ the distance between the sensor node and the LPU.

- *Path Communication Loss*: Path communication loss is defined as the power loss due to transmission from

This article has been accepted for publication in a future issue of this journal, but has not been fully edited. Content may change prior to final publication. Citation information: DOI 10.1109/TMC.2018.2822279, IEEE Transactions on Mobile Computing

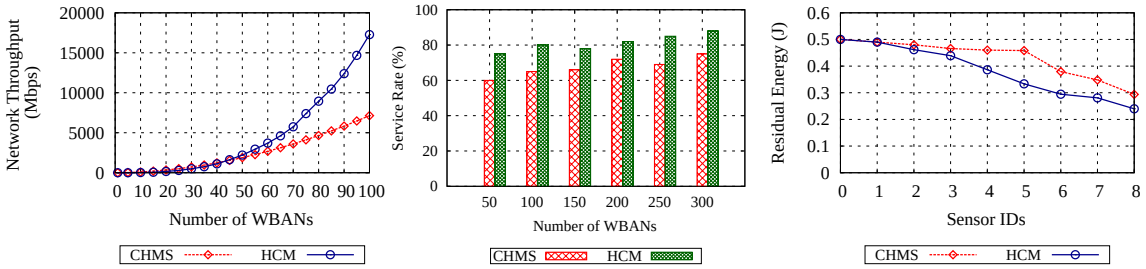

(a) Network Throughput (b) Service Rate (c) Residual Energy

Figure 5: Analysis of throughput, service rate, and residual energy

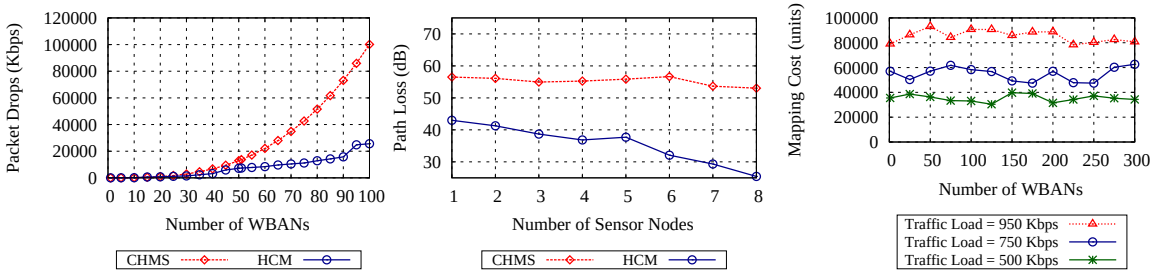

(a) Number of Packets Drop (b) Path Loss (c) Mapping Cost

Figure 6: Analysis of packet drop, path loss, and mapping cost

sensor node to the reception in the LPU [45].

$$PL(dB) = 10\Xi \log_{10}(\frac{\mathcal{D}_0}{\mathcal{D}}) + 10\log_{10}\frac{(4\pi\mathcal{D}_0)^2}{\lambda} + X\sigma \quad (72)$$

where Ξ is the path loss exponent varying between $2-3.5$, $\mathcal{D}$ denotes the distance among body sensor and LPU, $\mathcal{D}_0$ is the actual distance among body sensor and LPU, σ is the Gaussian variance, and X is the Gaussian random variable. The operating frequency is 2.4 GHZ.

8.4 Discussion on Results

We considered the proposed algorithm — HCM to analyze the performance, based on different simulation metrics.

8.4.1 Energy Consumption

Figure 3 depicts the energy consumption of WBANs for the proposed scheme. From the figure, we can see that with the increase in the number of HCSPs, the energy consumption of the critical WBANs decreases. In our proposed scheme, the critical WBANs form a DPG and are efficiently mapped to an optimal H-CSP. Therefore, the critical WBANs consume reduced energy than the normal WBANs, while transmitting the packets. With the increase in the number of H-CSPs, the energy consumption of each WBAN decreases. We also compare our existing work O-MAP with the Without Optimal Mapping Scheme (WoP) and existing scheme CHMS (considered to be normal), in which HCM outperforms the WoP and normal scheme (CHMS).

8.4.2 Total Number of Connected WBANs

Figure 4 depicts the total number of connected WBANs to optimal H-CSP in a critical emergency situation. We analyzed the proposed scheme with varying number of WBANs 100, 150, and 200 and varying number of H-CSPs 5, 10, and 15. Figures 4(a), 4(b), and 4(c) depict that the total number of served WBANs is more than the existing scheme based on the available bandwidths of the H-CSPs. On the other hand, from the figures, we can observe that with the increase in the number of H-CSPs, the total number of served WBANs from an particular H-CSP increases. Therefore, the critical WBAN can get improved services in the presence of multiple H-CSPs. We also compared our scheme with the exiting solution, and observe that our scheme outperforms the existing one.

8.4.3 Communication Path Loss

Figure 6(b) depicts the cumulative path loss of sensor nodes with two schemes — CHMS and HCM. We measured the path loss using Equation (72), where the path exponent varies from $3-4.5$, and the operating frequency 2.4 GHz. In the presence of group-based mobility, the distance between the sensor nodes and LPUs increases over time, which increases the path loss of body sensor. Therefore, to minimize the power consumption, it is very important to minimize the path loss. As the proposed scheme manages the mobility of WBANs by charging an extra amount for mobility management, therefore it minimizes the path loss. Hence, we observe that the HCM significantly minimizes the path loss of sensor nodes over the existing schemes.

8.4.4 Packet Loss

Figure 6(a) shows the mean packet loss of WBANs for different schemes — CHMS and HCM. Due to group-based mobility of WBANs, the quality of channel between sensor nodes and LPUs decreases significantly, which increases the packet loss the exciting system. The proposed scheme provides an optima and efficient between WBANs and H-CSPs, which inherently decreases the packet loss rate of the system and provides fair resources to sensor nodes. Therefore, the proposed scheme, HCM, reduces the packet loss, while maintaining the QoS requirements of WBANs. The scheme used in HCM, able to provide fair performance than the existing schemes CHMS, as they do not consider QoS requirements of the WBANs.

This article has been accepted for publication in a future issue of this journal, but has not been fully edited. Content may change prior to final publication. Citation information: DOI 10.1109/TMC.2018.2822279, IEEE Transactions on Mobile Computing

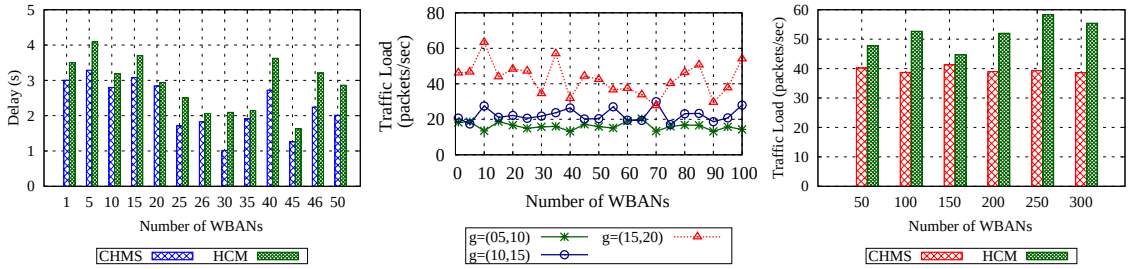

(a) Average Delay (b) Traffic Load with varying in density (c) Traffic Load

Figure 7: Analysis of average delay, traffic load with variation in the density and traffic load

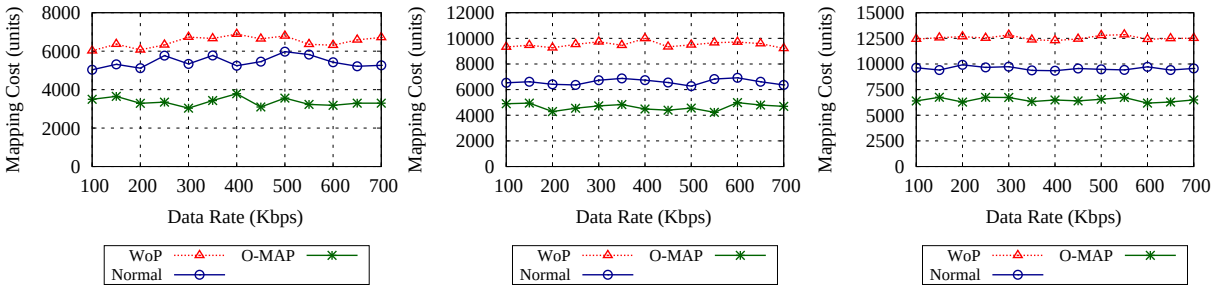

(a) Number of WBANs: 100 (b) Number of WBANs: 200 (c) Number of WBANs: 300

Figure 8: Mapping cost with with variation in number of WBANs

8.4.5 Network Throughput

Figure 5(a) presents the mean throughput of WBANs for HCM and CHMS. Throughput is the reception of the packets successfully at the AP. As previously mentioned, throughput depends on the number of successful reception of packets at the sink. Therefore, due to the increase of alive nodes in the network, the packet reception rate increases. As a result, the network throughput increases due to the increase of alive nodes. From 5(a), we can observe that using HCM, the WBANs from a DPG are efficiently mapped to the H-CSP, which maximizes the packet transmission rate. Consequently, as WBANs carry sensitive and important medical data packets, therefore it is necessary to increase the throughput of WBANs in efficient way, where our proposed approach provides significant improvement in throughput for critical WBANs. Therefore, the proposed scheme HCM has less packet drop rate compared to CHMS.

8.4.6 Service Rate

Figure 5(c) shows the service rate of the H-CSP for HCM and CHMS. We have calculated the service rate using Equation 70. In our proposed scheme, the WBANs are mapped to H-CSP efficiently while considering the traffic load. Therefore, the service rate of the proposed scheme is $5 - 10\%$ more than that of the existing scheme. Hence, we observe that the proposed scheme, HCM, outperforms the existing scheme CHMS, as the latter does not consider the efficient mapping of WBANs to H-CSP.

8.4.7 Residual Energy

Figure 5(c) depicts the energy levels of WBANs for HCM and CHMS. Each WBAN struggles to transmit its data packets. Nevertheless, due to mobility of the WBANs, the packet transmission rate decreases and the WBAN consumes more energy. As a result, the residual energy of the WBAN decreases. In our proposed scheme, due to efficient mapping of critical WBANs to H-CSP, each WBAN connects to optimal H-CSP, while preserving the QoS requirement and providing fair amount of resources. Therefore, for the efficient mapping and data transmission, the HCM scheme consumes less energy. Therefore, the proposed scheme, HCM, outruns the existing scheme CHMS, as the latter does not consider the efficient mapping of WBANs to H-CSP.

8.4.8 Packet Delivery Delay

Figure 7(a) describes the packet delivery delay from WBAN to AP. In this figure, we observe that using the proposed scheme, the critical WBANs have less packet delivery delay than the normal WBANs. As, in our scheme, the critical WBANs are efficiently mapped to the H-CSP, therefore the WBANs can send their data immediately. Therefore, efficient mapping incurs less packet delivery delay using HCM. However, we observe that the HCM scheme, outruns the scheme CHMS, as the latter does not consider the efficient mapping of WBANs to H-CSP.

8.4.9 Traffic Load

Fig. 7(b) depicts the traffic capacity of cloud-assisted WBANs. From Fig. 7(c), we can observe that with the increase in the density g of WBANs, the traffic volume increases, which significantly decreases the network performance. To cope with the situation, our proposed algorithm deals with the increase in traffic load and provides QoS to each WBAN. From Fig. 7(b), we can see that our proposed scheme HCM decreases the increased traffic load in a medical emergency situation.

8.4.10 Reliability

To calculate the reliability of the proposed scheme, we used the elastic reliability optimization technique proposed by Zhao *et al.* [46]. Figure 9(a) presents the reliability of the proposed scheme with the variation in the number of WBANs. From the

This article has been accepted for publication in a future issue of this journal, but has not been fully edited. Content may change prior to final publication. Citation information: DOI 10.1109/TMC.2018.2822279, IEEE Transactions on Mobile Computing

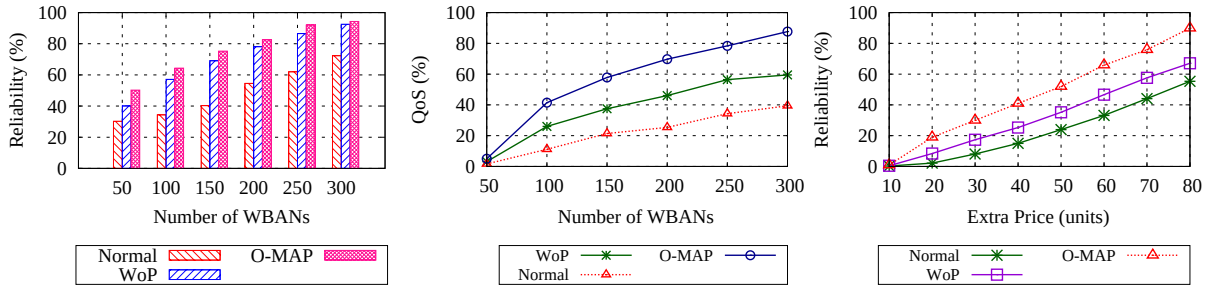

(a) Reliability (b) QoS (c) Reliability

Figure 9: Analysis of reliability and QoS

figure, we observe that the reliability of the system increases with the increase in the number of WBANs. Our proposed scheme uses the optimal mapping technique between WBANs and CSPs, while taking into consideration of interference management price for the minimization of interference among coexisting WBANs. Therefore, if any WBAN fails to function in the presence of other coexisting WBANs and/or other radio technologies, the H-CSPs charge an extra price to minimize the effects of the interference. As a result, our proposed approach provides higher reliability than the existing schemes. Figure 9(c) shows the reliability with the variation in extra price in the network. Here, we vary the extra price within the range $10-80$ units. From the figure, we observe that the reliability of WBANs increases with the increase in the extra price. The mutual and cross technology interference among WBANs is accounted for by the extra charge. Therefore, as the extra price increases, the interference among WBANs decreases, and the reliability increases. Consequently, the proposed scheme achieves higher reliability than the existing approaches.

8.4.11 QoS

Figure 9(b) presents the QoS of the proposed scheme with varying number of WBANs in a medical emergency situation. From the figure, we observe that QoS increases using the proposed approach – O-MAP. As the O-MAP scheme proposes efficient mapping between WBANs and H-CSPs, the service delay of the network decreases. Consequently, the successful packet transmission rate increases. As a result, the QoS of the network also increases. We also compared our proposed scheme in the normal and WoP scenario. We observe that the proposed scheme outperforms the existing others.

8.4.12 Mapping Cost

Figure 6(c) shows the mapping cost of WBANs for different traffic load in a medical emergency situation. From the figure, we observe that with the increase of traffic load the mapping cost of WBANs increases significantly. On the other hand, the traffic load of 950 Kbps incurs more mapping cost than the traffic load of 750 Kbps. To cope with the increased mapping cost for optimal mapping between WBANs and H-CSPs, we provide an optimal mapping algorithm — O-MAP. Figure 8 depicts the mapping cost between WBANs and H-CSPs for different data rates of body sensor nodes. From this figure, we observe that the mapping cost using the proposed approach — O-MAP — is lesser than that without optimal mapping — WoP — and the conventional approach (CHMS).

9 Conclusion

Increased traffic load in an area decreases the performance of the network with respect to the mapping cost and the mean network throughput. Therefore, to minimize the traffic load, we proposed a disease-centric relation estimation approach to optimize the computational complexity of cluster formation. After estimation of the relation among WBANs, we proposed an algorithm to form DPG, considering several disease types such as epidemic cholera, glandular fever, and epidemic parotitis. DPG alone is not sufficient to provide QoS services to the WBANs. Therefore, we also proposed another algorithm for efficient mapping of WBANs belonging to a DPG with an optimal H-CSP. We performed the complexity analysis and stability of the proposed algorithm. We also compared our proposed schemes with the existing schemes, from which we are able to show that our approach outperforms the existing approaches we considered as the benchmarks and achieves significant results.

In the future, we plan to analyze the dynamic behavior of WBANs in a critical emergency situation and also propose a dynamic cache optimization scheme for handling such emergency situation. Also, we plan to design an optimal and effective resource augmentation process in WBANs for edge computing platform [47].

References

[1] T. Hayajneh, G. Almashaqbeh, S. Ullah, and A. V. Vasilakos, "A Survey of Wireless Technologies Coexistence in WBAN: Analysis and Open Research Issues," *Wireless Networks*, vol. 20, no. 8, pp. 2165–2199, 2014.

[2] G. Fortino, G. Di Fatta, M. Pathan, and A. Vasilakos, "Cloud-Assisted Body Area Networks: State-of-the-Art and Future Challenges," *Wireless Networks*, vol. 20, no. 7, pp. 1925–1938, 2014.

[3] M. Chen, S. Gonzalez, A. Vasilakos, H. Cao, and V. C. Leung, "Body Area Networks: A Survey," *Mobile Networks and Applications*, vol. 16, no. 2, pp. 171–193, 2011.

[4] A. Argyriou, A. C. Breva, and M. Aoun, "Optimizing Data Forwarding from Body Area Networks in the Presence of Body Shadowing with Dual Wireless Technology Nodes," *IEEE Transactions on Mobile Computing*, vol. 14, no. 3, pp. 632–645, 2015.

[5] G. E. Santagati and T. Melodia, "Experimental Evaluation of Impulsive Ultrasonic Intra-Body Communications for Implantable Biomedical Devices," *IEEE Transactions on Mobile Computing*, vol. PP, no. 99, pp. 1–1, 2016.

[6] P. Rakovic and B. Lutovac, "A Cloud Computing Architecture with Wireless Body Area Network for Professional Athletes Health Monitoring in Sports Organizations – Case Study of Montenegro," in *Proceedings of Mediterranean Conference on Embedded Computing*, 2015, pp. 387–390.

[7] A. Abbas and S. U. Khan, "A Review on the State-of-the-Art Privacy-Preserving Approaches in the e-health Clouds," *IEEE Journal of Biomedical and Health Informatics*, vol. 18, no. 4, pp. 1431–1441, 2014.

[8] B. E. Reddy, T. S. Kumar, and G. Ramu, "An Efficient Cloud Framework for Health Care Monitoring System," in *Proceedings of International Symposium on Cloud and Services Computing*, 2012, pp. 113–117.

[9] G. Ferna'ndez, I. de la Torre-Diez, and J. J. Rodrigues, "Analysis of the Cloud Computing Paradigm on Mobile Health Records Systems," in *Proceedings of International Conference on Innovative Mobile and Internet Services in Ubiquitous Computing*, 2012, pp. 927–932.

[10] S. Ullah, K. Pervez, N. Ullah, S. Saleem, H. Higgins, K. S. Kwak *et al.*, "A Review of Wireless Body Area Networks for Medical Applications," *International Journal of Communications, Network and System Sciences*, vol. 2, no. 08, p. 797, 2009.

[11] G. Fortino, D. Parisi, V. Pirrone, and G. D. Fatta, "BodyCloud: A SaaS Approach for Community Body Sensor Networks," *Future Generation Computer Systems*, vol. 35, no. 0, pp. 62–79, 2014.

[12] M. Quwaider and Y. Jararweh, "Cloudlet-Based Efficient Data Collection in Wireless Body Area Networks ," *Simulation Modelling Practice and Theory*, vol. 50, no. 0, pp. 57–71, 2015.

[13] F. Zhang, J. Cao, S. U. Khan, K. Li, and K. Hwang, "A Task-Level Adaptive MapReduce Framework for Real-Time Streaming Data in Healthcare Applications," *Future Generation Computer Systems*, vol. 43, pp. 149–160, 2015.

[14] M. Chen, "NDNC-BAN: Supporting Rich Media Healthcare Services via Named Data Networking in Cloud-Assisted Wireless Body Area Networks," *Information Sciences*, vol. 284, no. 0, pp. 142–156, 2014.

[15] O. Diallo, J. J. Rodrigues, M. Sene, and J. Niu, "Real-Time Query Processing Optimization for Cloud-based Wireless Body Area Networks," *Information Sciences*, vol. 284, no. 0, pp. 84–94, 2014.

[16] E. Rachkidi, E. H. Cherkaoui, M. Ait-idir, N. Agoulmine, N. C. Taher, M. Santos, and S. Fernandes, "Cooperative Dynamic eHealth Service Placement in Mobile Cloud Computing," in *Proceedings of International Conference on E-health Networking, Application Services*, 2015, pp. 627–632.

[17] A. Abbas and S. U. Khan, "e-Health Cloud: Privacy Concerns and Mitigation Strategies," in *Medical Data Privacy Handbook*. Springer, 2015, pp. 389–421.

[18] G. V. Prasad, A. S. Prasad, and S. Rao, "A Combinatorial Auction Mechanism for Multiple Resource Procurement in Cloud Computing," *IEEE Transactions on Cloud Computing*, vol. PP, no. 99, pp. 1–1, 2016.

[19] L. Zhou, Z. Yang, J. J. P. C. Rodrigues, and M. Guizani, "Exploring Blind Online Scheduling for Mobile Cloud Multimedia Services," *IEEE Wireless Communications*, vol. 20, no. 3, pp. 54–61, 2013.

[20] A. Samanta, S. Misra, and M. S. Obidat, "Wireless Body Area Networks with Varying Traffic in Epidemic Medical Emergency Sitaution," in *Proceedings of IEEE International Conference on Communications*, 2015, pp. 6929–6934.

[21] A. Samanta, S. Bera, and S. Misra, "Link-Quality-Aware Resource Allocation With Load Balance in Wireless Body Area Networks," *IEEE Systems Journal*, vol. 12, no. 1, pp. 74–81, 2018.

[22] A. Samanta and S. Misra, "Energy-Efficient and Distributed Network Management Cost Minimization in Opportunistic Wireless Body Area Networks," *IEEE Transactions on Mobile Computing*, vol. 17, no. 2, pp. 376–389, 2018.

[23] ——, "EReM: Energy-Efficient Resource Management in Body Area Networks with Fault Tolerance," in *Proceedings of IEEE Global Communications Conference*, 2017.

[24] E. Ibarra, A. Antonopoulos, E. Kartsakli, J. J. Rodrigues, and C. Verikoukis, "Joint Power-QoS Control Scheme for Energy Harvesting Body Sensor Nodes," in *Proceedings of IEEE International Conference on Communications*, 2014, pp. 3511–3516.

[25] M. Chen, Y. Ma, S. Ullah, W. Cai, and E. Song, "ROCHAS: Robotics and Cloud-assisted Healthcare System for Empty Nester," in *Proceedings of International Conference on Body Area Networks*, 2013, pp. 217–220.

[26] G. Kulkarni, R. Shelke, P. B. N. Patil, V. Kulkarni, and S. Mohite, "Optimization in Mobile Cloud Computing for Cloud Based Health Application," in *Proceedings of International Conference on Communication Systems and Network Technologies*, 2014, pp. 569–572.

[27] S. Wasserman, *Social Network Analysis: Methods and Applications*. Cambridge University Press, 1994, vol. 8.

[28] S. Ullah, H. Higgins, B. Braem, B. Latre, C. Blondia, I. Moerman, S. Saleem, Z. Rahman, and K. S. Kwak, "A Comprehensive Survey of Wireless Body Area Networks," *Journal of Medical Systems*, vol. 36, no. 3, pp. 1065–1094, 2012.

[29] N. Karowski, A. C. Viana, and A. Wolisz, "Optimized Asynchronous Multichannel Discovery of IEEE 802.15.4-Based Wireless Personal Area Networks," *IEEE Transactions on Mobile Computing*, vol. 12, no. 10, pp. 1972–1985, 2013.

[30] Y. Zhang, C.-H. Feng, I. Demirkol, and W. B. Heinzelman, "Energy-efficient duty cycle assignment for receiver-based convergecast in wireless sensor networks," in *Proceedings of IEEE Global Telecommunications Conference*, 2010, pp. 1–5.

[31] A. Kamel, A. Al-Fuqaha, and M. Guizani, "Exploiting Client-Side Collected Measurements to Perform QoS Assessment of IaaS," *IEEE Transactions on Mobile Computing*, vol. 14, no. 9, pp. 1876–1887, 2015.

[32] S. Ren and M. van der Schaar, "Dynamic Scheduling and Pricing in Wireless Cloud Computing," *IEEE Transactions on Mobile Computing*, vol. 13, no. 10, pp. 2283–2292, 2014.

[33] N. A. Nuaimi, A. A. Shamsi, N. Mohamed, and J. Al-Jaroodi, "e-Health Cloud Implementation Issues and Efforts," in *Proceedings of International Conference on Industrial Engineering and Operations Management*, 2015, pp. 1–10.

[34] Q. Chen, S. Kanhere, and M. Hassan, "Analysis of Per-node Traffic Load in Multi-hop Wireless Sensor Networks," *IEEE Transactions on Wireless Communications*, vol. 8, no. 2, pp. 958–967, Feb 2009.

[35] V. Kantere, D. Dash, G. Francois, S. Kyriakopoulou, and A. Ailamaki, "Optimal Service Pricing for a Cloud Cache," *IEEE Transactions on Knowledge and Data Engineering*, vol. 23, no. 9, pp. 1345–1358, 2011.

[36] S. Moulik, S. Misra, and A. Gaurav, "Cost-Effective Mapping between Wireless Body Area Networks and Cloud Service Providers based on Multi-Stage Bargaining," *IEEE Transactions on Mobile Computing*, vol. 16, no. 6, pp. 1573–1586, 2017.

[37] S. Misra and S. Sarkar, "Priority-Based Time-Slot Allocation in Wireless Body Area Networks During Medical Emergency Situations: An Evolutionary Game Theoretic Perspective," *IEEE Journal of Biomedical and Health Informatics*, vol. PP, no. 99, pp. 1–1, 2014.

[38] P. Wang and X. Du, "QoS-aware Service Selection Using An Incentive Mechanism," *IEEE Transactions on Services Computing*, vol. PP, no. 99, pp. 1–1, 2016.

[39] G. Almashaqbeh, T. Hayajneh, and A. Vasilakos, "A Cloud-Based Interference-Aware Remote Health Monitoring System for Non-hospitalized Patients," in *Proceedings of IEEE Global Communications Conference*, 2014, pp. 2436–2441.

[40] M. Nabi, M. Geilen, and T. Basten, "MoBAN: A Configurable Mobility Model for Wireless Body Area Networks," in *Proceedings of International Conference on Simulation Tools and Techniques*, 2011, pp. 168–177.

[41] X. Cai, J. Li, J. Yuan, W. Zhu, and Q. Wu, "Energy-Aware Adaptive Topology Adjustment in Wireless Body Area Networks," *Telecommunication Systems*, vol. 58, no. 2, pp. 139–152, 2015.

[42] A. Samanta, Y. Li, and S. Chen, "QoS-Aware Heuristic Scheduling with Delay-Constraint for WBSNs," in *Proceedings of IEEE International Conference on Communications*, 2018.

[43] A. Samanta and S. Misra, "Dynamic Connectivity Establishment and Cooperative Scheduling for QoS-Aware Wireless Body Area Networks," *IEEE Transactions on Mobile Computing*, vol. PP, no. 99, pp. 1–1, 2018.

[44] D. D. Guglielmo, F. Restuccia, G. Anastasi, M. Conti, and S. Das, "Accurate and Efficient Modeling of 802.15.4 Unslotted CSMA/CA through Event Chains Computation," *IEEE Transactions on Mobile Computing*, vol. PP, no. 99, pp. 1–1, 2016.

[45] M. Sandhu, N. Javaid, M. Akbar, F. Najeeb, U. Qasim, and Z. Khan, "FEEL: Forwarding Data Energy Efficiently with Load Balancing in Wireless Body Area Networks," in *Proceedings of IEEE International Conference on Advanced Information Networking and Applications*, 2014, pp. 783–789.

[46] J. Zhao, Y. Xiang, T. Lan, H. H. Huang, and S. Subramaniam, "Elastic Reliability Optimization Through Peer-to-Peer Checkpointing in Cloud Computing," *IEEE Transactions on Parallel and Distributed Systems*, vol. 28, no. 2, pp. 491–502, 2017.

[47] A. Samanta and Y. Li, "DeServE: Delay-agnostic Service Offloading in Mobile Edge Clouds: Poster," in *Proceedings of ACM/IEEE Symposium on Edge Computing*, 2017, pp. 24:1–24:2.